Optimizing the Geometric Parameters of Cutting Edge for Finishing Machining of 30Cr2Ni4MoV Alloy Steel

***F. Jiang[1], T.K. Liao[1], H. Xie[3], F.Z. Wang[1] and L. Yan[2]**

[1] Institute of Manufacturing Engineering, Huaqiao University, China.
[2] Machine Tool Factory, Dongfang Turbine Co., Ltd., China.
[3] College of Mechanical Engineering and Automation, Huaqiao University, China.

* jiangfeng@hqu.edu.cn

Abstract

In order to optimize the geometric parameters of cutting edge for finishing machining of 30Cr2Ni4MoV (30Cr) alloy steel, a 2D finite element (FE) model of orthogonal cutting has been built with FE software AdvantEdge. The optimized methodology of cutting edge geometric parameters has been proposed based on simulated results. Then, the geometric parameters of cutting edge have been optimized based on a comprehensive criterion combining chip deformation coefficient and tool stress. The chip deformation coefficient indirectly determines the surface roughness and tool stress determines tool wear, which affect the dimensional precision of parts. The range of rake angle is selected from 12° to 20° and the range of cutting edge radius is selected from 12μm to 20μm in the optimization process. The optimal rake angle for finishing machining 30Cr alloy steel is 16° and the optimal cutting edge radius is 14μm with given relief angle of 7°.

Keywords: Numerical simulation, Finishing machining, Chip deformation coefficient, Tool stress, Geometric parameters of cutting edge

Introduction

The deformation of workpiece material mainly depends on the cutting edge geometries, including rake angle, relief angle and edge radius which have great effect on flow stress, chip morphology and machined surface quality. Metal machining process is generally divided into rough and finishing machining. Rough machining pays more attention to the tool life while finishing machining pays more attention to the machining surface quality and tool wear.

Theoretical calculation or cutting experiments is difficult to determine the optimal cutting tool geometry quickly and effectively due to the complexity and instability of the cutting process. The machining process is thermo-mechanical coupled process. The finite element method (FEM) has been proven to be a useful tool to analyze the metal cutting process [1, 2] and optimize the process parameters [3, 4]. Many researchers focus on the optimization of cutting edge geometric parameters based on the FEM. In the previous research of our team, X. Cheng et al. [5] built the FE model to optimize the geometric parameters of cutting edge for rough machining of Fe-Cr-Ni stainless steel. The optimized methodology of cutting edge geometric parameters has been proposed, and the optimized methodology is based on the stress, and the cutting parameters are designed based on the equal material removal rate. Keyvan and E.Ng [6] used a combined empirical-numerical (FE) approach for predicting the tool life. This approach is based on the similarities found among the worn cutting edge geometries which have been obtained from the orthogonal tool life tests at different cutting speeds.

However, few studies have used the numerical simulation technology to optimize the parameters of cutting processes or cutting tools for machined surface quality. The main reason is that, the mesh size and remesh process or inputting unstable factors such as material failure of FEM model affect the formation process of machined surface in the cutting simulation. But the indirect indexes, chip deformation coefficient, obtained from numerical simulation analysis could be used in the optimization of machined surface quality. Related research pointed out that the chip morphology indirectly reflects the machined surface quality. The smaller chip deformation coefficient is, the better machined surface quality is. Su. G et al. [7] have found the correlations between chip morphology and machined surface micro-topography at different chip serration stages encountered in high speed cutting, and get a conclusion that the principal factor influencing surface roughness is the thickness of the sawed segment (tooth) of saw-tooth chip. Schultheiss et al. [8] have present a new model for predicting the surface roughness during turning operations, while the influence of the minimum chip thickness on the obtained surface roughness have been analyzed.

In this paper, a 2D FE model of orthogonal cutting process of 30Cr alloy steel has been built with commercial software Third Wave AdvantEdge. The temperature and stress and chip thickness under different cutting edge geometric parameters have been obtained. The influence of rake angle and cutting edge radius on the stress and chip deformation coefficient has been analyzed. A comprehensive criterion has been used in this paper, which is combining the chip deformation coefficient and stress. The chip deformation coefficient could reflect the machined surface quality while the tool stress could reflect the tool wear. Through this criterion, the rake angle and cutting edge radius of finishing machining 30Cr alloy steel have been optimized.

Nomenclature

f	feed rate	γ_0	rake angle
m	the strain rate hardening coefficient	ε_0	reference strain
n	the strain hardening coefficient	ε_s	actual stress
T	current deformation temperature	ρ_s	the density of specimen
v	cutting speed	σ_0	yield stress at reference strain
σ	tool stress	σ_s	flow stress
Λ	the comprehensive coefficient	ζ_a	the deformation coefficient
a_c	undeformed thickness	ξ_f	the factor of feed rate determine minimum element size
a_{ch}	chip thickness	ξ_r	the factor of cutting edge radius determine minimum element size
a_p	depth of cut	ΔT	the adiabatic temperature rise
c_0-c_3	the coefficient of heat softening	$\bar{\sigma}$	average of tool stress
C_1 C_2	the coefficient of normalization	S'_f	feed rate to determine minimum element size
C_p	the specific heat capacity of workpiece	S'_{min}	preset minimum element size
r_e	cutting edge radius	S'_r	cutting edge radius to determine minimum element size
S_{max}	maximum element size	$\dot{\varepsilon}_0$	reference strain rate
S_{min}	actual minimum element size	$\dot{\varepsilon}_s$	actual stress rate
T_{ini}	the initial deformation temperature	$\bar{\zeta}_a$	average of deformation coefficient
α_0	relief angle		

Model of orthogonal cutting 30Cr alloy steel

30Cr alloy steel used in the turbine rotor of the steam turbine and other key industrial areas. After hardening and tempering methods or high-frequency surface hardening, the comprehensive mechanical properties have been improved. The hardness is about 270HV.

The chemical compositions of 30Cr alloy steel are listed in Tab. 1. The microstructure of the material is shown in Fig. 1.

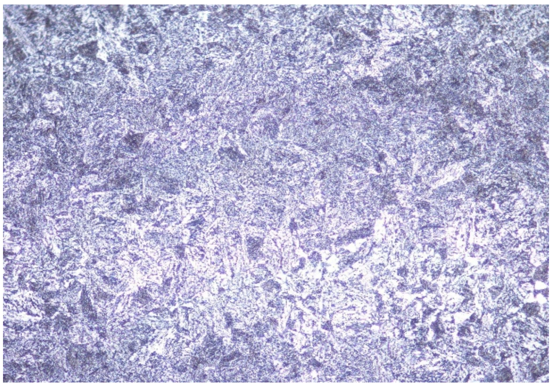

Figure 1. Microstructure of 30Cr alloy steel (500×)

Table 1. Chemical compositions of 30Cr alloy steel (wt.%)

Composition	C	Si	Mn	P	S	Ni	Cr	Mo	V	Fe
Content (wt.%)	≤0.35	≤0.03	≤0.05	≤0.004	≤0.002	1.6	3.5	0.3	0.08	Bal.

Cutting parameters of finishing machining

In the practical machining process, the cutting speed, feed rate and depth of cut could be varied in a reasonable range. It is essential to optimize the rake angle and cutting edge radius considering different cutting parameters with limited range. Lower cutting depth and feed and higher cutting speed have been generally used in finishing machining process. In order to obtain the optimal value of rake angle and cutting edge radius with a good adaptability, the process parameters are set in a reasonable range. The machining parameters are listed in the Tab. 2.

Table 2. Finishing machining cutting parameters

a_p (mm)	f (mm/rev)	v (m/min)	Number (No.)
1	0.1	100	1
		140	2
		180	3
	0.15	100	4
		140	5
		180	6
	0.2	100	7
		140	8
		180	9

Cutting speed is set at 3 levels and feed rate is also set at 3 levels. The depth of cut is set as 1mm in all simulations. In this paper, the single-factor design of experiment has been used, so there are 9 combinations of finishing machining cutting parameters.

The simplified model and meshing control

Simulations have been performed with AdvantEdge which integrates advanced FE models appropriate for machining operations. Assuming the workpiece material is isotropic, the material is removed in same state at all times. Besides, each point of cutting edge is equivalent in the direction of cutting depth.

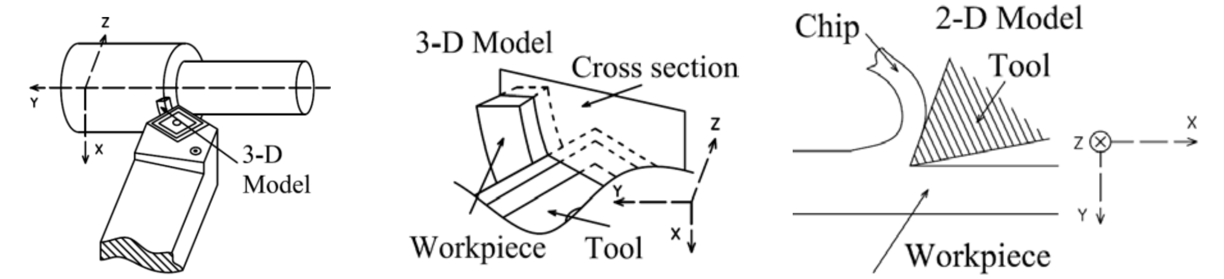

(a) turning process (3D) (b) 3D model (c) 2D plane strain problem

Figure 2. A complex 3D problem transforms into a simple 2D plane strain problem

Therefore, a complex three-dimensional (3D) problem, as shown in Fig.2 (a) and (b), transforms into a simple two-dimensional (2D) plane strain problem as shown in Fig.2 (c). In this model, cutting tool is regarded as rigid and applied by fully constrained in a non-contact surface. In the 2D plane strain model, the workpiece moves in X direction with the cutting speed while the tool is fixed, and the feed direction translate into Y direction, as shown in Fig.2 (c).

The deformation of the material will cause the mesh distortion during the process of FE simulation. The adaptive FE mesh is the important features of the AdvantEdge software, therefore, it not only solve the above problems, but also improve the accuracy for the edge region after refinement processing and ensures the calculation efficiency for the region away from the cutting edge after coarsening processing.

Mesh grading (0.1~1.0) determine the nature of the transition from fine elements near the cutting edge to coarse elements away from the cutting edge. Increasing this parameter will result in a more coarsen mesh. In this study, the mesh grading is set to 0.4.

The workpiece meshing parameters, the mesh coarsening factor and the mesh refinement factor are set to 6 and 2 respectively; S_{max} is set to 0.1mm, and S'_{min} is set to 0.02mm; S'_f defines the smallest element length through the chip thickness, thus, the factor ξ_f setting in the study is use as default 0.1; S'_r defines the element length in the vicinity of the cutting edge. In order to keep minimum element size of all models be built by the same standard, the factor ξ_r setting in the study is 0.4. In this way, the minimum element size of all models is determined by the cutting edge radius. The FE model with mesh is shown in Fig. 3.

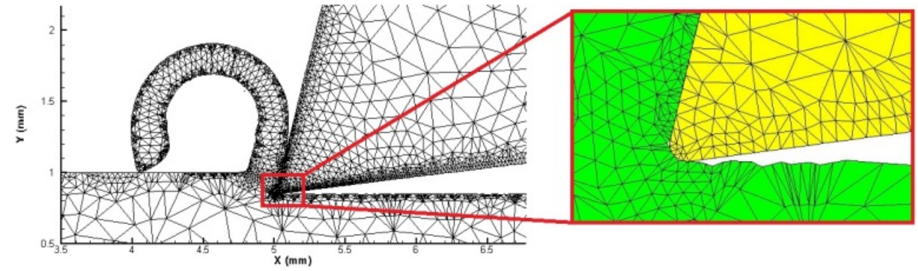

Figure 3. Finite element model with mesh

The method of how to ensure the minimum element size of all models with the same standard is as follows: for example, there are 3 kinds of feed rate (f_1, f_2, f_3) and 6 kinds of cutting edge radius (r_{e1}, r_{e2}, r_{e3}, r_{e4}, r_{e5}, r_{e6}) in this study. In order to keep the minimum element size of all models be determined by the cutting edge radius, it should be pay more attention to adjusting the value of ξ_r to make the S_{min} equal to S'_r.

$$S'_r = \xi_r \cdot max(r_{e1}, r_{e2}, r_{e3}, r_{e4}, r_{e5}, r_{e6}) \quad (1)$$

$$S'_f = \xi_f \cdot min\left(f_1, f_2, f_3\right) \quad (2)$$

$$S_{min} = min\left(S'_r, S'_f, S'_{min}\right) \quad (3)$$

Material constitutive model and friction mode

The numerical simulation of metal cutting involves many models, such as friction model [9], material constitutive model [10], heat transfer model and thermal physical property model [11]. Material constitutive model has been modified continuously to form the thermal-mechanical coupling phenomenon and the iterative process of the algorithm. When the thermal-mechanical coupling reaches the equilibrium and the cutting simulation process reaches the steady state, the system output the final results which include the cutting stress, chip deformation and other physical quantities. It could be seen that the key models for the numerical simulation of metal cutting is the material constitutive model.

Material constitutive model is a set of equations that reflect the stress-strain relationship of the deformable body material [12]. At present, the spilt Hopkinson pressure bar (SHPB) technique is usually used to determine the flow stress and strain data in a certain range of strain rate and temperature [13]. According to these data and the corresponding empirical formula, the constitutive equation is established. There are many types of constitutive equations of materials [14], power-law (P-L) constitutive model has been introduced the strain hardening, strain rate hardening and thermal softening parameters, which is a comprehensive reflection of large strain, high strain rate and high temperature load [15]. At the same time, it is simple in its own form and applied to a variety of computer encoding, so it is a practical model for analysis and calculation of. The P-L constitutive model is expressed as [16]:

$$\sigma_s=\sigma_0\left(1+\frac{\varepsilon_s}{\varepsilon_0}\right)^{1/n}\times\left(1+\frac{\dot{\varepsilon}_s}{\dot{\varepsilon}_0}\right)^{1/m}\times\left(c_0+c_1T+c_2T^2+c_3T^3\right) \tag{4}$$

$$T=T_{ini}+\Delta T \tag{5}$$

$$\Delta T=\frac{1}{\rho_s C_p}\int\sigma_s \mathrm{d}\varepsilon_s \tag{6}$$

The SHPB technique has been used to study the dynamic deformation behavior of 30Cr alloy steel. The true stress-true strain curves of workpiece material have been obtained. The P-L model constitutive model is given as the following [17]:

$$\sigma_s=547.92\left(1+\frac{\varepsilon_s}{0.01}\right)^{1/8.9047}\times\left(1+\frac{\dot{\varepsilon}_s}{100}\right)^{1/6.9979}\times(1.0308\text{-}1.8124e^{-3}T+2.1826e^{-6}T^2\text{-}1.2745e^{-9}T^3 \tag{7}$$

σ_s (MPa), $\dot{\varepsilon}_s$ (s^{-1}), T (℃).

Comprehensive criterion combining chip deformation coefficient and tool stress

AdvantEdge utilizes Tecplot software to display and assist in analyzing simulation results. The average stress in the tool can be computed and obtained easily. The stress history is average over the highest 10% of the elements in the cutting tool, as show in the Fig. 4. Then, the average of stress history which has achieved steady state is calculated as a quantitative data.

However, the quality of machined surface is difficult to be observed directly from the 2D FE model, and the surface quality has great relationship with chip deformation coefficient in the finishing machining process. Generally small chip deformation coefficient means small material deformation in the cutting process, which result in better surface quality. Thus, the chip deformation coefficient is proposed as an indirect index to evaluate the machined surface quality. The deformation coefficient of workpiece can be calculated as follows:

$$\zeta_a=\frac{a_{ch}}{a_c} \tag{9}$$

The ac is the undeformed thickness, which is equal to the feed rate in the 2D FE model. Chip thickness is obtained by measuring the radius of a circle which the center at the inner side of the chip, and the circle are tangent to the outer side of the chip. In order to ensure the accuracy of the measured chip thickness, the chip thickness is measured 6 times and the average value is obtained, as show in the Fig. 5.

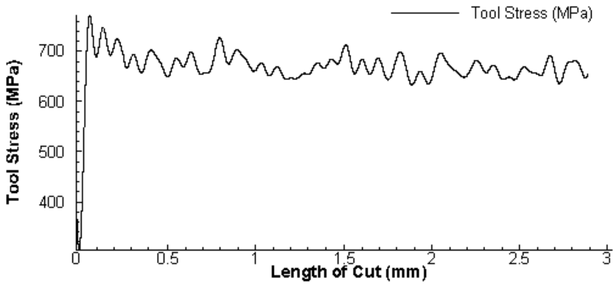

Figure 4. Average over the highest 10% of the elements in the cutting tool

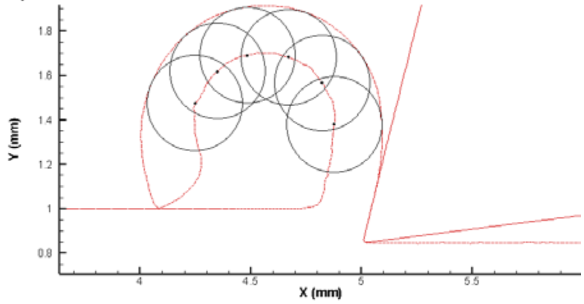

Figure 5. Schematic illustration of measuring chip thickness

The comprehensive criterion combining deformation coefficient and stress is expressed as:

$$\Lambda = C_1 \frac{\zeta_a}{\bar{\zeta}_a} + C_2 \frac{\sigma}{\bar{\sigma}} \tag{10}$$

The determination of C_1, C_2, $\bar{\zeta}_a$ and $\bar{\sigma}$ is as follow:

Assuming the simulation results of different cutting edge radius with one rake angle are show in the Tab. 3. The method of comprehensive criterion to optimize the cutting edge radius as follows:

The values of $\Lambda_1 \sim \Lambda_5$ are compared, and the minimum value of the corresponding cutting edge radius is the optimal under this rake angle. The method of comprehensive criterion to optimize the rake angle is the same as mentioned above.

Table 3. Simulation results of different cutting edge radius with one rake angle

cutting edge radius(μm)	12	14	16	18	20
stress(MPa)	σ_1	σ_2	σ_3	σ_4	σ_5
deformation coefficient	ζ_{a1}	ζ_{a2}	ζ_{a3}	ζ_{a4}	ζ_{a5}

$$\bar{\sigma} = \frac{\sigma_1 + \sigma_2 + \sigma_3 + \sigma_4 + \sigma_5}{5} \tag{11}$$

$$\bar{\zeta}_a = \frac{\zeta_{a1} + \zeta_{a2} + \zeta_{a3} + \zeta_{a4} + \zeta_{a5}}{5} \tag{12}$$

$$\Delta\sigma = \max\left(\frac{\sigma_n}{\bar{\sigma}}\right) - \min\left(\frac{\sigma_n}{\bar{\sigma}}\right) \tag{13}$$

$$\Delta\zeta_a = \max\left(\frac{\zeta_{an}}{\bar{\zeta}_a}\right) - \min\left(\frac{\zeta_{an}}{\bar{\zeta}_a}\right) \tag{14}$$

$$C_1=\frac{\Delta\sigma}{\Delta\sigma+\Delta\zeta_a} \qquad (15)$$

$$C_2=\frac{\Delta\zeta_a}{\Delta\sigma+\Delta\zeta_a} \qquad (16)$$

$$\Lambda_n=c_1\frac{\zeta_{an}}{\bar{\zeta}_a}+c_2\frac{\sigma_n}{\bar{\sigma}} \qquad n=1,2,3,4,5 \qquad (17)$$

Optimization procedures

According to the characteristics of geometric parameters of cutting tool, the optimization procedures are proposed. Relief angle (α_0) impacts the contact length between the machined surface and flank face of tool. A reasonable relief angle for finishing machining is 5°~8° [18]. According to the carbide indexable inserts design standards [19], relief angle of 7° is select. In the process of finishing, the cutting tool wear and machined surface quality are more important. Larger rake angle (γ_0) can get a better machined surface quality, while excessively rake angle not only weakens the cutting edge strength, but also reduce the cutting edge of the volume and lead to the increase of cutting tool wear, which lower the dimensional precision. At the same time, the deformation coefficient decreases with the increase of the rake angle. Therefore, it is an optimal rake angle to balance the tool stress and the deformation coefficient. Larger cutting edge radius (r_e) gets a smaller tool stress but increases the chip deformation coefficient, while smaller cutting edge radius gets smaller chip deformation coefficient but increases the tool stress. Thus, it is an optimal cutting edge radius to balance the tool stress and the deformation coefficient for the specific process parameters and specific materials.

According to reference [17], 12°~20° is the reasonable range for rake angle and 12μm~20μm is the reasonable range for cutting edge radius in the finishing machining process. The optimization steps are shown in ANNEX A, and the numbers of cutting parameter are shown in Tab. 2.

Step 1: The optimization process is divided into two parts, one is the optimization of the rake angle, and the other is the optimization of the cutting edge radius. The two are respectively independent and not related to each other.

Step 2: 9 sets of cutting parameters are mentioned above. In each set of cutting parameters, all of the rake angle and cutting edge radius should be carried crossover. The rake angle is changed from 12° to 20° with interval of 2° and a total of 5 values (12°, 14°, 16°, 18°, 20°) are selected; the cutting edge radius is changed from 12μm to 20μm with interval of 2μm and a total of 5 values (12μm, 14μm, 16μm, 18μm, 20μm) are selected. Therefore, there are 225 sets of simulations to be performed.

Step 3: 2 optimal rake angles are obtained according to the comprehensive criterion of 225 sets of simulations, while 2 optimal cutting edge radiuses are also obtained. Finally, the 4 sets of combination with 2 optimal rake angles and 2 optimal cutting edge radiuses are obtained.

Step 4: The optimal combination of cutting edge geometric parameters is obtained through the comprehensive criterion which based on the above 4 sets of combination.

The simulated results

Summary of optimal cutting edge geometric parameters

A total of 45 optimal cutting edge radiuses are obtained in 5 different rake angles while based on 9 sets of cutting parameters in the Tab. 4. The value of each column is obtained by the fixed rake angle and changed cutting edge radius with 9 sets of cutting parameter based on the comprehensive criterion. Then the total number obtained by summing the number of each cutting edge radius, and the total number of the first two will be elected to alternative area.

Table 4. Summary of optimal cutting edge radius

Number as optimal value		Rake angle 12°	14°	16°	18°	20°	Total(45)
Cutting edge radius	12μm	4	5	4	4	3	20
	14μm	3	2	2	3	3	13
	16μm	1	0	2	1	1	5
	18μm	1	0	0	0	0	1
	20μm	0	2	1	1	2	6

A total of 45 optimal rake angles are obtained in 5 different cutting edge radiuses while based on 9 sets of cutting parameters in the Tab. 5. The value of each line is obtained by the fixed cutting edge radius and changed rake angle with 9 sets of cutting parameter based on the comprehensive criterion. Then the total number obtained by summing the number of each rake angle, and the total number of the first two will be elected to alternative area.

Table 5. Summary of optimal rake angle

Number as optimal value		Rake angle 12°	14°	16°	18°	20°
Cutting edge radius	12μm	0	4	5	0	0
	14μm	0	4	5	0	0
	16μm	0	1	4	3	1
	18μm	1	3	4	1	0
	20μm	0	0	7	0	2
Total (45)		1	12	25	4	3

It can be seen obviously in Tab. 4. and Tab. 5. In a series of cutting edge radius, the number of 12μm and 14μm are higher, and the number of the 14° and 16° in a series of rake angles are higher, too. Therefore, 4 sets of optimization combination are obtained by the cross combination of 2 rake angle and 2 cutting edge radius. These 4 combinations are as follows: 14°-12μm, 14°-14μm, 16°-12μm, 16°-14μm (fixed relief angle is 7°)

The optimal combination of cutting edge geometric parameters was determined

Table 6. New addition of machining cutting parameters

a_p (mm)	f (mm/rev)	v (m/min)	Number (No.)
1	0.08	120	10
		160	11
		200	12
	0.13	120	13
		160	14
		200	15
	0.18	120	16
		160	17
		200	18

In order to ensure the correctness of the optimization results, 3 sets of feed rate (0.08mm/rev, 0.13mm/rev, 0.18mm/rev) and 3 sets of cutting speed (120m/min, 160m/min, 200m/min) are added to carry out the additional simulation experiment for these 4 combinations. Thus, a total of 36 new simulation experiments are given. The new machining cutting parameters are list in the Tab. 6.

Then, a total of 4 combinations of rake angle and cutting edge radius are obtained under 18 sets of cutting parameters respectively and the total number of the first will be elected to be the optimal combination of cutting edge geometric parameters. The 4 combinations of rake angle and cutting edge radius are listed in the Tab. 7. It can be seen obviously that the third combination, 16°-14μm, is the optimal.

Analysis on contours of temperature and stress

Several combinations of cutting edge geometric parameters were taken as examples to analyze the contours of temperature and stress.

As shown in Fig.6, it can be seen obvious change in the stress distribution of the tool with the increase of rake angle and little change with the increase of cutting edge radius. Increasing rake angle results in the highest values of stress expand to the flank face of insert. But the stress of the primary deformation is increasing with the increase of cutting edge radius.

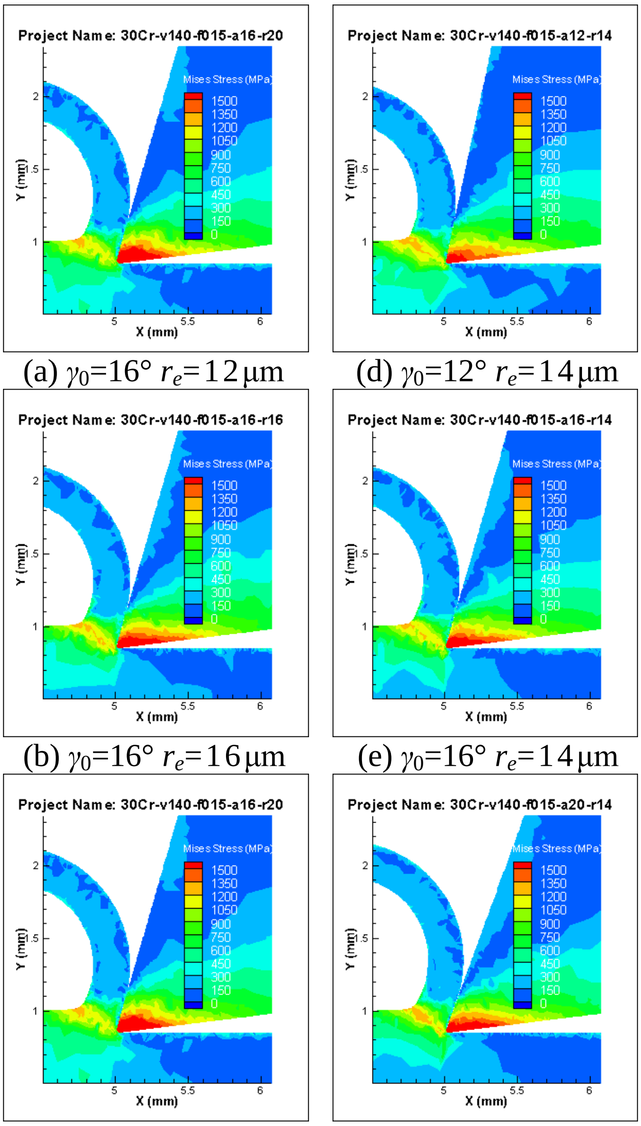

(a) γ_0=16° r_e=12μm (d) γ_0=12° r_e=14μm

(b) γ_0=16° r_e=16μm (e) γ_0=16° r_e=14μm

(c) γ_0=16° r_e=20μm (f) γ_0=20° r_e=14μm

Figure 6. The contours of stress in different combination (v=140m/min f=0.15mm/rev a_p=1mm α_0= 7°)

Table 7. Optimal combination of rake angle and cutting edge radius

4 combinations	The number of cutting parameters 1	2	3	4	5	6	7	8	9	10	11	12	13	14	15	16	17	18	Total
14°-12μm				*										*				*	2
14°-14μm																			0
16°-12μm					*	*	*						*			*	*	*	7
16°-14μm	*	*	*					*	*	*	*	*			*				9

The meaning of "*" in the Tab.8 is that the combination of this cutting edge radius and rake angle is optimal for this set of cutting parameters.

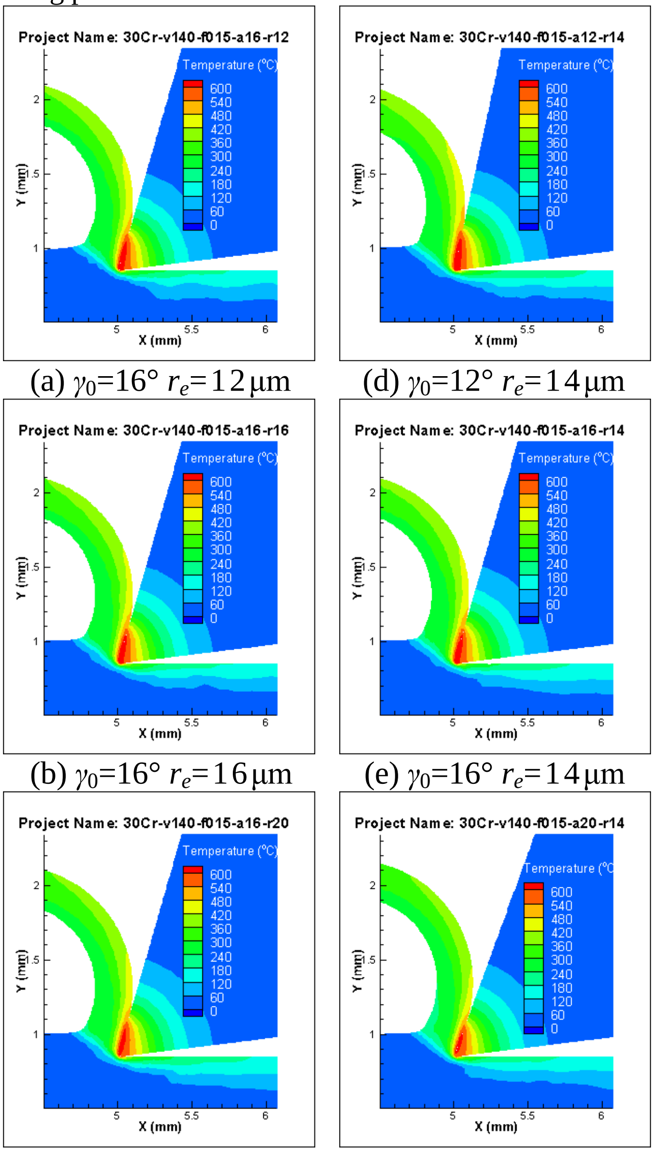

(a) γ_0=16° r_e=12μm (d) γ_0=12° r_e=14μm

(b) γ_0=16° r_e=16μm (e) γ_0=16° r_e=14μm

(c) γ_0=16° r_e=20μm (f) γ_0=20° r_e=14μm

Figure 7. The contours of temperature in different combination (v=140m/min f=0.15mm/rev a_p=1mm α_0= 7°)

As shown in Fig. 7 there is no obvious change in the temperature distribution of the tool and primary deformation zone with the change of the rake angle and cutting edge radius.

Conclusions

In this paper, a 2D FE model of orthogonal cutting 30Cr alloy steel has been built to analyze the deformation coefficient and stress under different cutting edge geometric parameters. The rake angle and cutting edge radius for finishing machining Fe-Cr-Ni alloy steel have been optimized. The conclusions are as follows:

In the finishing machining 30Cr alloy steel, the cutting edge geometric parameters have greater influence on stress than temperature.

The optimized methodology of cutting edge geometric parameters has been proposed which is a comprehensive criterion combining chip deformation coefficient and tool stress.

In the finishing machining 30Cr alloy steel, the optimal rake angle 16°, and the optimal cutting edge radius is 14μm when the relief angle is fixed 7°. The correctness of the optimized results can be guaranteed by a uniform comprehensive criterion and multiple sets of validation experiments.

Acknowledgments

This research is sponsored by the National Natural Science Foundation of China (No.51475173), the Major Project on the Integration of Industry and Research of Fujian Province (No.2014H6018), the Research and Innovation Ability of Graduate Students in Huaqiao University (No.1511403008).

References

[1] Atlati, S., B. Haddag, M. Nouari, and M. Zenasni. (2014). Thermomechanical modelling of the tool-workmaterial interface in machining and its implementation using the ABAQUS VUINTER subroutine. *INT J MECH SCI* **87:**102-117.

[2] Ben Moussa, N., H. Sidhom, and C. Braham. (2012). Numerical and experimental analysis of residual stress and plastic strain distributions in machined stainless steel. *INT J MECH SCI* **64:**82-93.

[3] Bharilya, R. K., R. Malgaya, L. Patidar, R. K. Gurjar, and A. K. Jha. (2015). Study of Optimised Process Parameters in Turning Operation Through Force Dynamometer on CNC Machine. *Materials Today: Proceedings* **2:**2300-2305.

[4] Krol, T. A., C. Seidel, and M. F. Zaeh. (2013). Prioritization of Process Parameters for an Efficient Optimisation of Additive Manufacturing by Means of a Finite Element Method. *Procedia CIRP* **12:**169-174.

[5] Cheng, X., X. Zha, and F. Jiang. (2016). Optimizing the geometric parameters of cutting edge for rough machining Fe-Cr-Ni stainless steel. *The International Journal of Advanced Manufacturing Technology* **85:** 683-693.

[6] Hosseinkhani, K., and E. Ng. (2015). A Combined Empirical and Numerical Approach for Tool Wear Prediction in Machining. *Procedia CIRP* **31:**304-309.

[7] Su, G., Z. Liu, L. Li, and B. Wang. (2015). Influences of chip serration on micro-topography of machined surface in high-speed cutting. *International Journal of Machine Tools and Manufacture* **89:**202-207.

[8] Schultheiss, F., S. R. H Gglund, V. Bushlya, J. Zhou, and J. St Hl. (2014). Influence of the Minimum Chip Thickness on the Obtained Surface Roughness During Turning Operations. *Procedia CIRP* **13:**67-71.

[9] Taureza, M., X. Song, and S. Castagne. (2014). Depth-dependent stress-strain relation for friction prediction. *INT J MECH SCI* **86:**46-53.

[10] Jiang, F., L. Yan, and Y. Rong. (2013). Orthogonal cutting of hardened AISI D2 steel with TiAlN-coated inserts simulations and experiments. *The International Journal of Advanced Manufacturing Technolog*y **64:**1555-1563.

[11] Jiang, F., T. Zhang, and L. Yan. (2016). Estimation of temperature-dependent heat transfer coefficients in near-dry cutting. *The International Journal of Advanced Manufacturing Technology.* **86:**1207-1218.

[12] Hu, W., Y. Lin, S. Yuan, and Z. He. (2015). Constitutive models for regression of various experimental stress-strain relations. *INT J MECH SCI* **101-102:**1-9.

[13] Malakizadi, A., S. Cedergren, I. Sadik, and L. Nyborg. (2016). Inverse identification of flow stress in metal cutting process using Response Surface Methodology. *SIMUL MODEL PRACT TH* **60:**40-53.

[14] Buchkremer, S., B. Wu, D. Lung, S. Münstermann, F. Klocke, and W. Bleck. (2014). FE-simulation of machining processes with a new material model. *J MATER PROCESS TECH* **214:**599-611.

[15] Jiang, F., J. Li, J. Sun, S. Zhang, Z. Wang, and L. Yan. (2010). Al7050-T7451 turning simulation based on the modified power-law material model. *The International Journal of Advanced Manufacturing Technology* **48:**881.

[16] Yu, J., F. Jiang, Y. Rong, H. Xie, and T. Suo. (2014). Numerical study the flow stress in the machining

process. *The International Journal of Advanced Manufacturing Technology* **74:**509-517.
[17] Xie, H., Yu, J., Wang, G., Rong, Y., Ye, J. and Liu, Y. (2016). Constitutive model for dynamic mechanical response of high strength steel. *Journal of Sichuan University (Nature Science Edition)* **53:**382-388.
[18] Trent, E. M., and P. K. Wright (2000). *Metal Cutting (Fourth Edition) in Book Metal Cutting (Fourth Edition) Butterworth-Heinemann Ltd; 4th Revised edition.*
[19] GB/T2076-2007 (ISO6987/1-1993). The Carbide Indexable Inserts Design Standards. *China National Standardization Management Committee.*